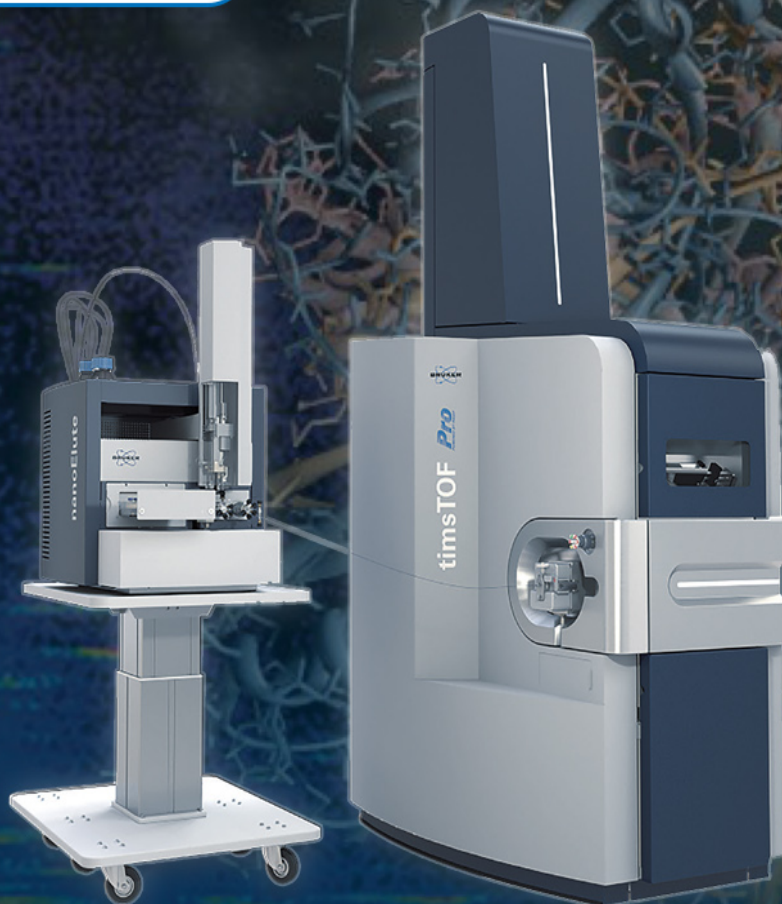




timsTOF Pro/fleX – Four reasons to switch to 4D-Proteomics™ on the timsTOF platform

If you are writing a grant and want some concise arguments for replacing older 3D mass spectrometers with the 4D capable on the timsTOF platform, download this brochure.

[Click Here to Download the Brochure](#)



Phillips Alexandra (Orcid ID: 0000-0001-5959-5238)

Compound-specific sulfur isotope analysis of cysteine and methionine via preparatory liquid chromatography and elemental analyzer isotope-ratio mass spectrometry

Alexandra A Phillips*, Fenfang Wu, Alex L Sessions

California Institute of Technology, Department of Geological and Planetary Sciences, Pasadena, CA, USA

*Corresponding author: alex.phillips@caltech.edu

ABSTRACT

Rationale: Compound-specific isotope analysis (CSIA) of organic sulfur molecules has previously been hindered by challenging preparatory chemistry and analytical requirements for large sample sizes. The natural-abundance sulfur isotopic compositions of the sulfur-containing amino acids, cysteine and methionine, have therefore not yet been investigated despite potential utility in biomedicine, ecology, oceanography, biogeochemistry, and other fields.

Methods: Cysteine and methionine were subjected to hot acid hydrolysis followed by quantitative oxidation in performic acid to yield cysteic acid and methionine sulfone. These stable, oxidized products were then separated by reverse-phase high performance liquid chromatography (HPLC) and verified via offline liquid chromatography mass spectrometry (LC/MS). The sulfur isotope ratios ($\delta^{34}\text{S}$ values) of purified analytes were then measured via combustion elemental analyzer coupled to isotope ratio mass spectrometry (EA/IRMS). The EA was equipped with a temperature-ramped chromatographic column and programmable He carrier flow rates.

Results: On-column focusing of SO_2 in the EA/IRMS system, combined with reduced He carrier flow during elution, greatly improved sensitivity allowing precise (0.1 - 0.3‰ 1s.d.) $\delta^{34}\text{S}$ measurements of 1 to 10 μg sulfur. We validated that our method for purification of cysteine and methionine was negligibly fractionating using amino acid and protein standards. Proof-of-concept measurements of fish muscle tissue and bacteria demonstrated differences up to 4‰ between the $\delta^{34}\text{S}$ values of cysteine and methionine that can be connected to biosynthetic pathways.

Conclusions: We have developed a sensitive, precise method for measuring the natural-abundance sulfur isotopic compositions of cysteine and methionine isolated from biological samples. This capability opens up diverse applications of sulfur isotopes in amino acids and proteins, from use as a tracer in organisms and the environment to fundamental aspects of metabolism and biosynthesis.

Keywords: Amino Acids, Cysteine, Methionine, Sulfur Isotopes, EA/IRMS, CSIA

This article has been accepted for publication and undergone full peer review but has not been through the copyediting, typesetting, pagination and proofreading process which may lead to differences between this version and the Version of Record. Please cite this article as doi: 10.1002/rcm.9007

1 | INTRODUCTION

The sulfur isotopic compositions of amino acids (AAs) are virtually unexplored but may hold significant utility across diverse scientific disciplines. In biomedicine, pilot studies have suggested that cysteine and methionine $\delta^{34}\text{S}$ values could indicate disease progression as sulfur metabolism is dysregulated at the onset of liver cancer¹. In archeology, bulk protein $\delta^{34}\text{S}$ measurements from mummy hair² and mammalian collagen³ have been used to reconstruct ancestral migration and reliance on fish protein, indicating this as a promising direction for targeted paleodiet reconstruction. Mass-balance isotopic models in plants suggest that differences related to metabolism could exist between cysteine and methionine $\delta^{34}\text{S}$ values, which in turn could inform agricultural sectors on the efficiency of sulfur uptake in soils⁴. Cysteine and methionine also have potential in biogeochemical studies to record redox conditions, for example direct incorporation of ^{34}S -depleted sulfide in anoxic sediments has been demonstrated in deep-reaching mangrove roots⁵. Measuring the compound-specific S isotope ratios of cysteine and methionine offer more powerful insights than would bulk protein analyses, disentangling the effects of metabolism versus environmental change. Here, we present the first method for natural-abundance sulfur isotope characterization of these amino acids, with successful measurements of 1-10 μg sulfur ($\sim 4\text{-}40$ μg analyte).

Progress towards the compound-specific isotopic analysis of organic sulfur compounds has historically been hindered by mass spectrometric limitations (Table 1). Sulfur isotope measurements typically relied on analyte combustion to SO_2 , a highly polar, toxic, corrosive, and hygroscopic gas, before online measurement via isotope ratio mass spectrometry (IRMS). To compensate for a host of analytical difficulties resulting from these properties of SO_2 , analyses required relatively large sample sizes ranging from 70 to 100 μg S even when using a specialized elemental analyzer (EA) with online combustion that improved on traditional dual-inlet designs⁶⁻⁷. Moreover, because the EA does not inherently separate different analyte compounds, offline preparative purification is needed prior to analysis. The combination of these two requirements presented a substantial barrier to measurements of analytes such as amino acids that exist in the environment in low concentrations. An alternative strategy for sulfur isotope determination used fluorination of analytes to sulfur hexafluoride (SF_6), which required large sample sizes but improved the precision due to the favorable properties of SF_6 ⁸. When measurements of this inert gas were combined with a microvolume and tenfold-increased signal amplification, detection limits were lowered to 0.6-3.2 μg S⁹. However, the preparation of SF_6 requires specialized vacuum lines and dangerous reactants and has not yet been demonstrated for organic analytes⁹⁻¹¹. Multi-collector inductively coupled plasma mass spectrometry (MC/ICPMS) has also recently demonstrated remarkably low sensitivity for measuring the sulfur isotopes of sulfate and sulfur-bearing minerals¹²⁻¹³, but thus far requires conversion of analytes to sulfate. Direct coupling of gas chromatography (GC) to MC/ICPMS was first reported in 2009¹⁴, and has enabled highly sensitive, compound-specific measurements of organic sulfur compounds, including volatile species from crude oils¹⁴ and mature sediments¹⁵, as well as marine dimethylsulfonopropionate¹⁶ (DMSP). Unfortunately for our application, GC separation of cysteine and methionine is not a viable option because existing derivatization strategies are not reliably quantitative and may fractionate sulfur isotopes.

Simultaneous with ICPMS development, there has been a parallel renaissance in EA/IRMS technology leading to significantly reduced sample sizes: online 'purge and trap' configurations have measured 35-350 μg sulfur¹⁷ and dual-column GC systems have reached 30-70 μg sulfur¹⁸. Most recently, the Thermo Scientific Flash EA-Isolink equipped with a temperature-ramped chromatographic column measured $\delta^{34}\text{S}$ in bone collagen samples containing just 2-3 μg sulfur¹⁹. This system, which we improved upon in the current study, provides sufficient sensitivity to make offline preparative isolation of the sulfur AAs much less tedious.

Analyses of cysteine and methionine have also faced significant difficulties in their chemical separation. Isolation methods have typically employed hot acid hydrolysis to release amino acid residues from proteins²⁰. However, this approach led to partial or complete oxidation of cysteine and methionine to cysteic acid and methionine sulfone (Figure 1), even when the headspace was flushed with argon or nitrogen gas²¹⁻²². To avoid such problems, amino acid residues were often oxidized²³⁻²⁵, reduced^{21,26-27}, or alkylated²⁸⁻³¹. However, alkylation only effectively targets cysteine, and reduction only methionine (Table S1, supporting information). Recent studies have thus converged on oxidation with performic acid (CH_2O_3) to quantitatively yield cysteic acid and methionine sulfone prior to LC/MS separation and quantification³²⁻³³.

Here we employed a modified version of this oxidation strategy. We validated the method as non-fractionating using commercial standards of cysteine, methionine, and bovine serum albumin (a well characterized, sulfur-rich protein), and established performance characteristics of the methodology. We then applied our novel approach to biomass from two ubiquitous microbes, *Escherichia coli* and *Pseudomonas fluorescens*, and to muscle tissue from two ecologically important fish species, *Oncorhynchus nerka* (salmon) and *Thunnus albacares* (tuna). These analyses revealed offsets of up to 4‰ in the cysteine and methionine $\delta^{34}\text{S}$ values that can probably be traced to metabolism. We expect that this new methodology will augment the growing stable isotope toolkit, with applications in biomedicine, ecology, agriculture, oceanography, biogeochemistry, and other diverse scientific fields.

2 | EXPERIMENTAL

2.1 | Method Overview

Samples were freeze dried then homogenized with mortar and pestle prior to acid hydrolysis (Figure 2). An aliquot was taken for bulk $\delta^{34}\text{S}$ analysis via EA/IRMS. Filtered, hydrolyzed AAs were then heated in performic acid, where cysteine and methionine were quantitatively oxidized to cysteic acid and methionine sulfone. Reverse-phase preparatory HPLC/UV was used to separate and purify the two sulfur AAs. Aliquots were assayed for purity via a separate LC/MS analysis. Further aliquots of the purified AA's were analyzed via EA/IRMS to measure $\delta^{34}\text{S}$ values.

2.2 | Experimental Reagents

Standards of cysteine, methionine, cysteic acid, methionine sulfone, and bovine serum albumin (BSA) were purchased from Sigma Aldrich (St. Louis, MO, USA; all >99% purity). All solvents used were ACS reagent grade, with the exception of ammonium hydroxide and ammonium acetate, which were HPLC grade. All water used was ultrapure (>18.2 M Ω). All glassware was combusted at 460 °C for seven

hours to remove organic carbon contamination. Vials and syringes were additionally washed with solvent before use (methanol, dichloromethane).

2.3 | Sample Preparation

Filets of wild-caught *O. nerka* (sockeye salmon) and *T. albacares* (yellowfin tuna) were purchased at a grocery store in Pasadena, CA, USA. Bacterial cultures (*E. coli*, *P. fluorescens*) were grown in our laboratory (details below). Biomass from all four was rinsed with water five times, then freeze dried with a VirTis lyophilizer (SP Scientific, Stone Ridge, NY, USA) for 1–3 days until dry (Figure 2, Step 1). Samples were transferred to a solvent-washed ceramic mortar and pestle and ground under liquid N₂ until homogenized (Figure 2, Step 2). Homogenized samples were then transferred to glass jars and 3 x 1 mg aliquots were taken for bulk $\delta^{34}\text{S}$ analysis via EA/IRMS (Figure 2, Step 3).

2.4 | Acid Hydrolysis

30 mg each of AA standards, BSA protein, and microbial biomass, and 100 mg of fish tissue were weighed directly into 60-mL vials. 10 mL of water was added and samples were sonicated for 15 min before the addition of 10 mL 12N HCl. Vials were placed on a hot plate in the fume hood (100 °C, 24 hrs; Figure 2, Step 4). Following hydrolysis, samples were vacuum filtered through baked Whatman GF/F glass fiber filters (0.7 μm pore size) and rinsed with water into new 60-mL vials. Filtered samples were dried to completion under a stream of N₂ in an acid-grade fume hood.

2.5 | Performic Acid Oxidation

Performic acid was prepared immediately prior to use by mixing hydrogen peroxide and formic acid in a 9:1 (v:v) ratio and incubating (30 min, 23 °C). 5-10 mL of performic acid was added to dried samples, which were placed on a hot plate (70 °C, 60 min) in the fume hood, with occasional stirring throughout the reaction before quenching on ice (Figure 2, Step 5). Oxidized samples were dried under a stream of N₂. Samples were then resuspended via vortexing in 1.5 mL ultrapure water and filtered through a 13 mm 0.22 μm PVDF (polyvinylidene fluoride) syringe filter (Millex) into a 2-mL vial for HPLC separation.

2.6 | HPLC/UV Separation

Methionine sulfone and cysteic acid were separated with an Agilent (Santa Clara, CA, USA) 1100 HPLC-UV system coupled to a Gilson (Middleton, WI, USA) FC203B fraction collector adapted from a previously described method³¹ (Figure 2, Step 6). Briefly, samples (100 μL) were separated on a PRPX100 strong anion exchange column (Hamilton, Reno, NV, USA) 250 mm x 4.6 mm x 5 μm , 30 °C) with isocratic 50 mM ammonium acetate, buffered to pH 8 with 25% ammonia solution, at a flow rate of 1.0 mL/min. Hydrolyzed samples produced a high and continuous background UV absorption signal, obscuring the peaks for cysteic acid and methionine. Fraction collection of samples was therefore based solely on time windows derived from separate analyses of methionine sulfone and cysteic acid standards monitored at 254 nm.

2.7 | LC/MS Verification

LC/MS analysis of all samples and standards was used to ensure that the collected analytes were pure. Fractions collected from HPLC-UV separation were derivatized with FDAA (1-fluoro-2-4-dinitrophenyl-5-L-alanine amide) and separated following a

previously published procedure³⁴ (Figure 2, Step 7). Briefly, 100 μL of aqueous sample was reacted with 10 μL of 6% triethylamine and 10 μL of 1% (w/v) FDAA in acetone at 50 °C for 60 min then quenched with 10 μL of 5% acetic acid. Aliquots (20 μL) were introduced to an Agilent 1100 Series LC/MSD with a Zobraz 300SB-CS column (Agilent, 2.1 mm x 150 mm x 5 μm), housed in the Caltech Proteomics Laboratory, for a 45 min gradient between 5% acetic acid and acetonitrile at a flow rate of 0.25 mL/min. Mass spectra were obtained in positive ion mode, scanning between m/z 300 and 450. The electrospray voltage was 4 kV at 350 °C. The diode array detector measured the UV absorption at 340 nm.

2.8 | EA/IRMS Measurement

Fractions collected from the HPLC-UV separation were transferred to tin capsules (OEA labs, Exeter, UK; 9mm x 5mm, pressed, ultra-clean) and dried overnight in an oven at 50 °C. Samples were analyzed with a Thermo Scientific (Bremen, Germany) EA IsoLink™ combustion elemental analyzer system coupled to a Delta V Plus Isotope Ratio Mass Spectrometer (Thermo Scientific) via a ConFlo IV Universal interface (Thermo Scientific, Figure 2, Step 8; Figure 3). The EA utilized a single-reactor configuration with user-packed columns comprising 3 cm of quartz wool, 14 cm wireform copper (5 mm size), 2 cm quartz wool, 6 cm granular tungsten (III) oxide, 1 cm quartz wool, and 0.5 cm additional tungsten (III) oxide. Sample combustion was accompanied by a pulse (4 s) of O_2 and carried in a high (100 mL/min) helium carrier gas flow rate. SO_2 is trapped on the GC column at 50°C, helping to sharpen the SO_2 peak while allowing CO_2 and N_2 to elute. The helium carrier flow is then reduced to 15 mL/min to improve the split ratios, and SO_2 is eluted as a sharp peak (<30 s FWHM) by ramping the GC column temperature to 240°C at 100°C/s. A typical IRMS measurement (24 min) brackets the sample SO_2 peak between four SO_2 reference gas peaks, with no magnet jump (Figure 4).

2.9 | Data Processing

The S contents (typically < 0.25 μg S) and $\delta^{34}\text{S}$ values (typically 1-10‰) of empty tin capsules were measured by EA/IRMS and used to correct all subsequent analyses for the blank contribution³⁵. Different batches of capsules varied in their S isotope composition by up to ~5‰ and therefore the same batch was used for all samples and standards within a day's run. In the current study this blank adjustment was minimal (< 5%) as sample peaks were sufficiently large (~30 Vs, 5 μg S); however, for smaller sample sizes the blank correction can become precision-limiting. A previous report concluded that oxygen isotope correction, i.e. for $^{32}\text{S}^{16}\text{O}^{18}\text{O}$, had a negligible effect on $\delta^{34}\text{S}$ values and therefore performed no explicit $\delta^{18}\text{O}$ correction¹⁹. In our data processing, any $\delta^{18}\text{O}$ effects are corrected for during calibration with external reference materials: $\delta^{34}\text{S}$ values were measured relative to a lab SO_2 reference gas that was itself calibrated against IAEA reference materials S1, S2, and S3 using the same EA/IRMS system. IAEA-S1 and IAEA-S2 standards were also analyzed in triplicate at the beginning, middle, and end of daily sequences to further calibrate sample $\delta^{34}\text{S}$ values, which were reported as permil (‰) variations relative to the Vienna Canyon Diablo Troilite (VCDT) reference frame.

Sayle et al¹⁹ observed large (0.6‰ per V) size-related errors for aliquots of bone collagen analyzed for $\delta^{34}\text{S}$ with the same model of EA/IRMS system. In our tests with SO_2 reference gas, performed daily prior to analyses, linearity effects were consistently low (<0.1‰ per V). We observed no significant size-related effects for

organic sulfur across a 3V range of signal intensities, except at very low sample sizes where blank contributions exceed 15%. This ~6x lower linearity dependence was potentially due to the less complicated sample matrices of purified AAs versus bone collagen. Low concentrations of cysteine and methionine in tissues precluded triplicate analyses of our proof-of-concept samples. The uncertainties for these analyses are therefore conservatively reported as <0.3‰, representing the poorest 1 σ precision encountered for any of the sulfur standard measurements, at the smallest concentration of 1 μ g sulfur (see method validation section for further details).

2.10 | Culturing Conditions

E. coli MG1655 and *P. fluorescens* WCS365 were grown in batch cultures on glucose in 1 L M9 minimal media that was modified to use ammonium sulfate as the sole sulfur source. The recipe was as follows: in 1L add 7.52 g Na₂HPO₄ • 2H₂O, 3.0 g KH₂PO₄, 0.5 g NaCl, 2.5 g (NH₄)₂SO₄, 1 mL 0.1 M CaCl₂, 1 mL 1.0 M MgCl₂, 4 g glucose, and 1 mL 1000x vitamins mix (DSM141 recipe). Initial inoculation occurred in 10-mL culture tubes before transfer to a 1 L Erlenmeyer flask. Cultures were kept at 37 °C on an Excella E24 Incubator Shaker Series (New Brunswick Scientific, Edison, NJ, USA) and grown overnight at 250 RPM. Cell growth was monitored by measuring OD₆₀₀ on a DU 800 UV/VIS spectrophotometer (Beckman Coulter, Brea, CA, USA). Cells were harvested in mid-log phase, at OD₆₀₀ ~1, and washed twice with 0.9% NaCl at 4 °C. Pellets were stored at -20 °C until analysis.

2.11 | Proton NMR

¹H NMR scans were performed on a Bruker (Bruker BioSpin, Rheinstetten, Germany) Avance III HD spectrometer with a Prodigy broadband cryoprobe (at 400 MHz). ~1 mg of sample was dissolved in D₂O in a Wilmad (Buena, NJ, USA) thin-walled high throughput NMR tube (Fisher Scientific, Hampton, NH, USA). 1D experiments were conducted with 64 scans (~5 min acquisitions) to increase signal to noise ratios.

3.0 | RESULTS AND DISCUSSION

3.1 | Method Development

Acid Hydrolysis

In early versions of method development, we first attempted to recover intact cysteine and methionine following acid hydrolysis, but were unable to achieve quantitative yields. Reported loss mechanisms for cysteine and methionine in typical acid hydrolysis conditions (100-110 °C, 6N HCl, 24 hrs) point to oxidation of the sulfur atom as the key process²² (Figure 1). To minimize such reactions, we carried out hydrolysis in closed ampules flushed with argon gas. While this successfully prevented any significant oxidation of methionine, ¹H NMR revealed ~5-10% conversion of cysteine to cysteic acid that presumably occurred during sample transfers and transient exposure to atmospheric O₂ (Figure S1, supporting information). Isotope fractionation ($\delta^{34}\text{S}$ change of ~1.6‰) of cysteine following anoxic hydrolysis was also observed, implying a kinetic isotope effect (KIE) for oxidation of roughly 15‰, assuming irreversible, closed-system behavior³⁵. Previous reports of acid hydrolysis under anoxic conditions echo these results, with up to 25% loss of cysteine²¹. Furthermore, although we did not observe methionine oxidation, others have noted significant conversion to methionine sulfoxide during sample storage and anoxic hydrolysis²¹. Given these problematic yields and apparent

isotopic fractionation, this strategy was abandoned in favor of quantitative oxidation of the AAs to more stable products prior to separation, as discussed next.

Performic Acid Oxidation

Oxidation of the sulfur atoms in cysteine and methionine – whether intentional or accidental – is liable to be fractionating, a fact reinforced by our acid hydrolysis experiments with cysteine. In pursuing a strategy of intentional oxidation it was therefore critical to ensure quantitative conversion. Sodium azide (NaN_3) has been suggested as a useful reagent, because it can be added directly to the hydrolysis mixture with little additional workup. However, yields of cysteic acid only reached 87%, which is insufficient conversion to mitigate isotope fractionation²⁴. Success in rapid oxidation of disulfides with hydrogen peroxide catalyzed by methyl trioxorhenium (MTO; CH_3ReO_3) has been demonstrated previously³⁶, but in our experiments methionine oxidation yields were incomplete and inconsistent, with a mixture of sulfoxide and sulfone products despite attempts to optimize reaction conditions (Figure S2, supporting information). MTO did yield quantitative oxidation of cysteine to cysteic acid, however. Performic acid oxidation, which has previously been reported to give near-quantitative yields for both cysteine and methionine²³, proved to be the most suitable for our needs. Increasing reaction time and temperature from the previously described 15 min incubation at 50°C, to 60 min at 70°C, resulted in quantitative yields within the limits of detection of ^1H NMR. Under these conditions, no cysteine, methionine, or methionine sulfoxide was detected in a triplicate experiment conducted on standards (Figure 5).

Ion-exchange Chromatography

Cation-exchange techniques are frequently employed in the isolation of AAs from environmental samples³⁷⁻³⁹ and could be beneficial to our application as a clean-up step. Unfortunately, the conventional strong cation exchange resin, Dowex 50WX8, employs a sulfonic acid functional group. Previous studies have concluded that significant column bleed probably results in the largest contribution to analytical blanks for isotope analysis of AAs⁴⁰. Given that no other commercial strong cation resins are available, we were forced to omit this typical step from our procedure, and instead limited clean-up to filtration through non-sulfur containing materials such as glass fiber filters and PVDF syringe filters. This does not present a significant limitation for analyses of pure biomass, as are presented here. However, for future work on more complex samples such as soils or sediments, this procedure should be revisited. In particular, sulfonic-acid stationary phase bleed may be resolved from the target analytes in the subsequent HPLC separation.

HPLC Separation

With cysteine and methionine in their native (unoxidized) form, we initially employed a reverse-phase Primesep A column (SIELC, Wheeling, IL, USA) for separating those analytes, following previously published methods specific to AA CSIA⁴¹ with hydrochloric acid substituted for sulfuric acid. However, after the decision to oxidize cysteine and methionine, two problems precluded further use of the Primesep A column. First, cysteic acid standards partially co-eluted with the void peak, despite method adjustments. Second, methionine sulfone standards co-eluted with cysteine, preventing the possibility of monitoring completion of the oxidation reaction via HPLC.

Cysteic acid and methionine sulfone were instead separated on a PRP X100 anion exchange column (Hamilton). Previous methods with this column used ICP/MS for sulfur-specific detection³¹, but such instrumentation was not available for our application, and is more complicated than necessary. We instead adapted the published separation to our HPLC-UV/Vis system, minimizing eluent ammonium acetate concentration due to UV absorption: the published 10 min gradient method between 25 and 250 mM ammonium acetate became a 20 min 50 mM isocratic run (Figure 6). One drawback to this isocratic method was the significant peak tailing of cysteic acid. Despite adjustments to flow rate, monitored wavelength, and eluent concentration, suboptimal peak shapes remained but as the compounds of interest were well resolved, we did not revisit this potential optimization. Further tests with cysteine, methionine, and sulfate confirmed that other sulfur-containing compounds did not coelute with cysteic acid or methionine sulfone.

LC/MS Verification

Due to the high absorption of protein components, the UV detector was saturated during sample runs. To verify that the correct analytes were collected, aliquots of each fraction were measured as their FDAA derivatives via electrospray ionization-LC/MS. Selected ion chromatograms were used to confirm the presence of derivatized cysteic acid (m/z 422) at 15.7 minutes and methionine sulfone (m/z 434) at 22.8 minutes (Figure 7). We used this procedure as a screening tool prior to EA/IRMS, only analyzing samples that had positive identification of the analyte and negative presence of the other AA residues. The procedure could also be used for quantification of the AAs, for example by using a heavy isotope labeled internal standard for calibration³⁴. FDAA has also been successfully used to determine the stereochemistry of AAs, even at trace concentrations (50 pmol)⁴²⁻⁴³.

Sulfur Isotopic Analysis by EA/IRMS

We made several attempts to measure cysteine and methionine $\delta^{34}\text{S}$ values by MC-ICPMS, as this approach would offer better sensitivity and higher precision than EA/IRMS, and concurrent measurement of $\delta^{33}\text{S}$ values. Given that matrix-matching of samples and standards is an important component of this analytical method, and that matrix effects have only been characterized for sulfate, we attempted to oxidize the sulfur amino acids to sulfate using hydrogen peroxide and UV light⁴⁴⁻⁴⁵. However, sulfate yields were low and variable when tested for cysteine ($43.5 \pm 10.1\%$, $n = 6$) and methionine ($21.5 \pm 3.5\%$, $n = 2$). Direct injection of sulfur amino acids into the ICP/MS system is theoretically possible but would require significant effort to matrix match standards and was not pursued. Use of GC/MC-ICPMS was precluded by the lack of a suitable derivatization strategy for cysteic acid⁴⁶, probably related to its negligible solubility in organic solvents. Indeed, our numerous attempts with various methylating and silylating agents produced no successful derivatives.

Ultimately, we decided to measure the sulfur amino acids by EA/IRMS, taking advantage of a new instrument with improved sensitivity. Two key improvements of this system were i) a temperature-ramped GC oven and ii) computer-controlled He flow rates (Figure 3). These modifications allowed SO_2 from combustion to have sharpened peak shapes and improved split ratios, as follows: during combustion mode, samples are burned ($>1020^\circ\text{C}$) with a pulse (4 s) of O_2 carried by a high helium carrier gas flow rate of 100 mL/min. The reactor contains an oxidizer catalyst of tungsten (III) oxide and a copper reducer which converts combustion gases to

NO_x, SO₂, CO₂, and H₂O. A water trap removes H₂O to prevent sulfuric acid formation. The copper digests extra oxygen from combustion and reduces NO_x species to N₂, and SO₃ to SO₂. In sulfur load mode, with the GC oven at 50 °C, N₂ and CO₂ are eluted and measured, but SO₂ is trapped in a narrow band on the column. Next, in sulfur measurement mode, the carrier gas flow rate is dropped to 15 mL/min to improve split ratios, while the GC temperature ramps to 240 °C releasing SO₂ as a sharp peak (<30 sec FWHM), improving signal to noise ratios. This flow rate of 15 mL/min represented the optimum choice for peak shape. Lower flow rates would improve split ratios further, but at the expense of greater SO₂ diffusion and therefore increased peak width and lower S/N ratios. Other explored parameters included timing of the GC heating cycle and sample combustion.

The default configuration for combined $\delta^{15}\text{N}$, $\delta^{13}\text{C}$, and $\delta^{34}\text{S}$ measurements by EA/IRMS includes a second reducing reactor, filled with copper shavings, to ensure complete conversion of NO_x species to N₂. In practice, including this additional reactor broadened SO₂ peak shapes significantly, and we therefore opted for the single reactor configuration. The previous characterization of this EA/IRMS system measured concurrent $\delta^{15}\text{N}$, $\delta^{13}\text{C}$, and $\delta^{34}\text{S}$ values of bone collagen also using a single reactor¹⁹. Without additional copper in the second reactor, however, there is potential for incomplete NO_x conversion to N₂, which was not explicitly tested for in their study. Although it is appealing to simultaneously measure all three isotope systems, to save time and expenses, we obtained the best precision for $\delta^{34}\text{S}$ values when only sulfur was analyzed. As our method focused on sulfur, we did not revisit combined analyses.

3.2 | Method Verification

Sensitivity and Precision of Isotopic Analyses

To characterize the sensitivity and precision of our improved EA/IRMS methodology, we measured in triplicate two inorganic and two organic sulfur standards (1 to 10 µg sulfur per aliquot): the silver sulfide standard IAEA-S1, seawater sulfate, cysteine acid, and methionine sulfone (Figure 8). Weighing standards at such low levels is challenging, so all but IAEA-S1 were dispensed volumetrically in aqueous solution, then dried in air at 50°C. The replicate precision (1 s.d.) for $\delta^{34}\text{S}$ values was < 0.20‰ for virtually all standards across this concentration range, rising to 0.30‰ only for the lowest level (1 µg S) of methionine sulfone. This result represents a decrease in sample size over a previous report focused on bone collagen, which reported analyses requiring 2 – 3 µg S, while at the same time improving on their average standard deviation of 0.3‰¹⁵. We believe that sensitivity and precision improvements are largely attributable to our advantages in running purified samples rather than archeological material and analyzing only sulfur rather than carbon and nitrogen simultaneously.

$\delta^{34}\text{S}$ Accuracy

Pure standards of cysteine and methionine were subjected to the entire amino acid separation procedure, with $\delta^{34}\text{S}$ measurements before and after, to examine the possibility of artifacts leading to sulfur isotope fractionations (Table 2). The initial $\delta^{34}\text{S}$ value of cysteine was $5.8 \pm 0.3\text{‰}$ and after acid hydrolysis, oxidation, and HPLC-UV separation, the value for the resultant cysteine acid was within error, $5.6 \pm 0.3\text{‰}$. Similarly, methionine had an initial $\delta^{34}\text{S}$ value of $7.4 \pm 0.3\text{‰}$ and a final methionine sulfone $\delta^{34}\text{S}$ value of $7.6 \pm 0.3\text{‰}$. Further verification using a pure

protein, bovine serum albumin (BSA), largely confirmed these results, but with a slight offset (0.4‰) between the reactant BSA protein and the product amino acids that falls within the 2σ limit (0.6‰) of analytical uncertainty (Table 2). Whether this offset represents random error, slight fractionation, or contamination of the parent BSA material (with, for example, trace amounts of sulfate) is unclear, but regardless, any fractionation induced is very small relative to the ~50‰ range of $\delta^{34}\text{S}$ values encountered in nature⁴⁷⁻⁴⁸.

3.3 | Pilot Samples

Biomass samples from the bacteria *E. coli* and *P. fluorescens*, and muscle tissue from the fish *O. nerka* and *T. albacares*, were analyzed for their compound-specific cysteine and methionine sulfur isotope ratios using the newly developed methodology (Figure 9).

Bulk Tissue Isotopic Compositions

P. fluorescens biomass $\delta^{34}\text{S}$ (2.3‰) was within error of its sulfur source, NH_4SO_4 , which was added to culture medium (2.1‰), while *E. coli* biomass was slightly ^{34}S -depleted (1.4‰). These minimal fractionations are consistent with previous reports that suggested offsets ranging from +0.5 to -4.4‰ between biomass and supplied sulfate for aquatic plants due to assimilatory sulfate reduction⁴⁹⁻⁵⁰. More recent studies measuring the $\delta^{34}\text{S}$ values of DMSP in phytoplankton and macroalgae suggest a smaller offset between sulfate and metabolites, between -1.4 to -2.8‰⁵¹. Our results, and future measurements of cysteine and methionine $\delta^{34}\text{S}$, add to these limited examples, expanding our understanding of the isotopic consequences of the understudied assimilatory pathway.

The $\delta^{13}\text{C}$ and $\delta^{15}\text{N}$ values of fish biomass are often related to food-chain position, with trophic effects expressed in consumers such as *O. nerka* and *T. albacares*. However, previous studies of trout suggest that $\delta^{34}\text{S}$ values do not track trophic levels, instead preserving the isotopic composition of local sulfate within ~2‰^{3,52-53}. Indeed, observed values for both *O. nerka* (19‰) and *T. albacares* (20‰) reflect marine sulfate (21‰¹²).

Cysteine and Methionine Isotopic Compositions

Compound-specific AA measurements were significantly more variable than the bulk biomass or muscle tissue measurements. For *E. coli*, the cysteine $\delta^{34}\text{S}$ value was 5.1‰ while the methionine value was 1.9‰. *P. fluorescens* exhibited the opposite pattern, with methionine enriched in ^{34}S with its $\delta^{34}\text{S}$ value at 4.8‰ relative to cysteine at 1.3‰. *O. nerka* and *T. albacares* had smaller differences between cysteine and methionine, although methionine was enriched in ^{34}S relative to cysteine in both species: the $\delta^{34}\text{S}$ values of *O. nerka* cysteine and methionine were 17.5‰ and 19.3‰, respectively, while in *T. albacares* cysteine was 17.0‰ and methionine was 18.2‰. Furthermore, although cysteine and methionine account for a large portion of cellular sulfur, the average isotope ratios of the two amino acids (cysteine, methionine) do not necessarily reflect bulk tissue values: for example, in *T. albacares*, both cysteine and methionine are ^{34}S -depleted compared with muscle tissue. As our method minimally or negligibly fractionates, these results imply the presence of other components of cellular sulfur with divergent $\delta^{34}\text{S}$ values, such as taurine, glutathione, sulfate esters, or inorganic sulfate stored in cells.

Heterogeneity in the cysteine and methionine $\delta^{34}\text{S}$ values implies further metabolic fractionations beyond the exogenous sulfur source (Figure 10). In fish, methionine is an essential amino acid that cannot be synthesized directly and must be acquired through dietary sources⁵⁴, which, as discussed earlier, are only minimally fractionating. Cysteine is produced from this methionine pool, through the intermediates, cystathionine and homocysteine⁵⁵. Given that methionine is not entirely converted to cysteine, this synthesis represents a branch point in metabolism that could express intrinsic isotope effects. We predict that a normal kinetic isotope effect (KIE) accompanies these reactions at the sulfur atom, which should leave the reactant, methionine, enriched relative to the product, cysteine, potentially explaining the patterns of enrichment which we observed in *O. nerka* and *T. albacares*. While this reaction has not explicitly been studied for the existence of isotope effects, early experiments using Raman spectroscopy suggest a 4-12‰ fractionation accompanying the nucleophilic addition of R-S⁻ groups^{4,56}, compatible with the observed offsets.

Unlike fish, *E. coli*, *P. fluorescens*, and most bacteria can synthesize *de novo* all twenty proteinogenic amino acids, including cysteine and methionine⁵⁷. However, bacterial sulfur AA synthesis is inherently more diverse, involving multiple potential pathways with distinct enzymes. In *E. coli*, cysteine biosynthesis proceeds by combining an activated homoserine intermediate with sulfide, the product of assimilatory sulfate reduction⁵⁸. Cysteine is then used as a substrate for methionine synthesis, through the transsulfuration pathway catalyzed by cystathionine γ -synthase and cystathionine β -lyase⁵⁹ (Figure 10, solid arrows). Alternatively, other bacteria, including multiple species of *Pseudomonas*, employ the sulfhydrylation pathway, which utilizes inorganic sulfide directly as the sulfur donor and the enzyme acylhomoserine sulfhydrylase⁵⁹ (Figure 12, dashed arrows). These different sulfur metabolisms offer a potential explanation for the contrasting patterns of *E. coli* and *P. fluorescens* cysteine and methionine $\delta^{34}\text{S}$ values. More specifically, the pattern of ^{34}S -enriched cysteine relative to methionine in *E. coli* can be understood as a result of the normal ^{34}S kinetic isotope effect of the transsulfuration pathway. Indeed, protein sulfur isotope studies and numerical models of higher plants, which use similar transsulfuration pathways, suggest that methionine is naturally ^{34}S depleted relative to cysteine⁴, as we observed in *E. coli*. In contrast, *P. fluorescens* must be enriching methionine in ^{34}S relative to cysteine. This is possibly occurring through the sulfhydrylation pathway, although details require further study. A third methionine synthesis pathway was recently discovered in freshwater and soil bacteria, although it is unlikely this nitrogenase-like enzyme is relevant here, as it is used only in sulfate limiting conditions⁶⁰.

4.0 | CONCLUSIONS

We have developed a novel approach to determining the natural-abundance $\delta^{34}\text{S}$ values of cysteine and methionine from biological samples. Acid hydrolysis followed by quantitative oxidation of the sulfur amino acids to their sulfone and sulfonic acid products with performic acid, results in air-stable analytes that can be further handled and purified. Separation was achieved via rapid (20 min) isocratic elution on a PRPX100 column and fraction purity was verified using derivatization with FDAA and characterization on an LC/MS system. Modifications to the operation of a Thermo Flash EA/IRMS system yielded substantially increased sensitive (1 to 10 μg sulfur) while maintaining precision (<0.3‰), enabling separation of measurable

aliquots in a single HPLC separation. Comparison of standard amino acids and BSA protein before and after sample processing indicates no significant methodological sulfur isotope fractionation. Proof-of-principle analyses of muscle tissue from two fish (*O. nerka* and *T. albacares*) found ^{34}S enrichment of methionine by $\sim 1\text{--}2\text{‰}$ relative to cysteine, in rough agreement with known metabolic KIEs. We found the opposite pattern in *E. coli*, with $\sim 3\text{‰}$ cysteine ^{34}S enrichment relative to methionine, probably due to fractionations in the transsulfuration synthesis pathway. The isotope patterns of *P. fluorescens* remained enigmatic, with methionine $\sim 4\text{‰}$ ^{34}S enriched relative to cysteine, a potential signature of the alternative synthesis via sulfhydrylation. Such heterogeneity in cysteine and methionine $\delta^{34}\text{S}$ values across diverse organisms holds much potential for further understanding of sulfur metabolism.

ACKNOWLEDGEMENTS

We would like to thank the technicians as well as the directors of the Proteomics Exploration Lab at Caltech: Sonja Hess and Anne Radimin for assistance with LC/MS operation and FDAA derivatization. This project benefited from the use of instrumentation made available by the Caltech Environmental Analysis Center and we acknowledge its director Nathan Dalleska for assistance with the HPLC-UV system. Caltech professors Victoria Orphan and Jess Adkins volunteered lab space for this project and we thank them and their lab technicians Stephanie Connon, Jared Markse, Grecia Lopez, and Guillaume Paris. We also thank high school interns Zekaria Beshir, Brenna Bowlen, and Hannah Betts for their valuable assistance on the project. We acknowledge Reto Wijker for providing cultures, media recipes, and assistance with microbial culturing. We thank colleagues for their valuable insight and review of early manuscripts: Ted Present, Preston Kemeny, Eryn Eitel, Hannah Dion-Kirschner, Frank Pavia, and Makayla Betts. We also thank Guillaume Tcherkez for procedures and advice on oxidation via MTO as well as Emilia Hernandez and Tony Wang for assistance testing oxidation of organics to sulfate. Tony Wang is also acknowledged for his help with optimizing initial EA/IRMS parameters. Funding for this project was provided by the NSF (Grant 1436566) and NASA Astrobiology Institute (Grant 80NSSC18M094).

REFERENCES

1. Albalat E, Telouk P, Balter V et al. Sulfur isotope analysis by MC-ICP-MS and application to small medical samples. *J Anal At Spectrom*. 2016;31(4):1002-1011. doi: 10.1039/C5JA00489F
2. Fourel F, Lecuyer C, Balter V. New frontiers for sulfur isotopic analysis. *Procedia Earth and Planetary Science*. 2015;13:232-239. doi: 10.1016/j.proeps.2015.07.055
3. Richards MP, Fuller BT, Hedges REM. Sulphur isotopic variation in ancient bone collagen from Europe: implications for human palaeodiet, residence mobility, and modern pollutant studies. *Earth Planet Sci Lett*. 2001;191(3):185-190. doi: 10.1016/S0012-821X(01)00427-7
4. Tcherkez G, Tea I. $^{32}\text{S}/^{34}\text{S}$ isotope fractionation in plant sulphur metabolism. *New Phytologist*. 2013;200:44-53. doi: 10.1111/nph.12314
5. Brunold C, Erismann KH. H_2S as sulfur source in *Lemna minor* L.: II. Direct incorporation into cysteine and inhibition of sulfate assimilation. *Experientia*. 1975;31:508-510. doi: 10.1007/BF01932426

6. Ueda A, Krouse HR. Direct conversion of sulphide and sulphate minerals to SO₂ for isotope analyses. *Geochemical Journal*. 1986;20:209-212. doi: 10.2343/geochemj.20.209
7. Glesemann A, Jager HJ, Norman AL, Krouse HR, Brand WA. On-line sulfur-isotope determination using an elemental analyzer coupled to a mass spectrometer. *Anal Chem*. 1994;66(18):2816-2819. doi: 10.1021/ac00090a005
8. Thode HG, Rees CE. Measurement of sulphur concentrations and the isotope ratios ³³S/³²S, ³⁴S/³²S, and ³⁶S/³²S in Apollo 12 samples. *Earth Planet Sci Lett*. 1971;12(4):434-438. doi: 10.1016/0012-821X(71)90029-X
9. Yang DA, Landais G, Assayag N, Widory D, Cartigny P. Improved analysis of micro- and nanomole- scale sulfur multi- isotope compositions by gas source isotope ratio mass spectrometry. *Rapid Commun Mass Spectrom*. 2016;30(7):897-907. doi: 10.1002/rcm.7513
10. Hulston JR, Thode HG. Variations in the S³³, S³⁴, and S³⁶ contents of meteorites and their relation to chemical and nuclear effects. *Journal of Geophysical Research*. 1965;70(4):3475-3484. doi: 10.1029/jz070i014p03475
11. Mayer B, Krouse HR. Procedures for sulfur isotope abundance studies. *Handbook of Stable Isotope Analytical Techniques*. 2004:538-596. doi: 10.1016/B978-044451114-0/50028-4
12. Paris G, Sessions AL, Subhas AV, Adkins JF. MC-ICP-MS measurement of δ³⁴S and Δ³³S in small amounts of dissolved sulfate. *Chem Geol*. 2013;345:50-61. doi: 10.1016/j.chemgeo.2013.02.022
13. Craddock PR, Rouxel OJ, Ball LA, Bach W. Sulfur isotope measurement of sulfate and sulfide by high-resolution MC-ICP-MS. *Chem Geol*. 2008;253:102-113. doi: 10.1016/j.chemgeo.2008.04.017
14. Amrani A, Sessions AL, Adkins JF. Compound-Specific δ³⁴S Analysis of Volatile Organics by Coupled GC/Multicollector-ICPMS. *Anal Chem*. 2009;81:9027-9034. doi: 10.1021/ac9016538
15. Raven MR, Adkins JF, Werne JP, Lyons TW, Sessions AL. Sulfur isotopic composition of individual organic compounds from Cariaco Basin sediments. *Org Geochem*. 2015;80:53-59. doi: 10.1016/j.orggeochem.2015.01.002
16. Amrani A, Said-Ahmad W, Shaked Y, Kiene RP. Sulfur isotope heterogeneity of oceanic DMSP and DMS. *PNAS*. 2013;110(46):413-418. doi: 10.1073/pnas.1312956110
17. Fourel F, Martineau F, Seris M, Lecuyer C. Simultaneous N, C, S stable isotope analyses using a new purge and trap elemental analyzer and an isotope ratio mass spectrometer. *Rapid Commun Mass Spectrom*. 2014;28:2587-2594. doi: 10.1002/rcm.7048
18. Fry B. Coupled N, C and S stable isotope measurements using a dual-column gas chromatography system. *Rapid Commun Mass Spectrom*. 2007;21(5):750-756. doi: 10.1002/rcm.2892
19. Sayle KL, Brodie CR, Cook GT, Hamilton WD. Sequential measurement of δ¹⁵N, δ¹³C and δ³⁴S values in archaeological bone collagen at the Scottish Universities Environmental Research Centre (SUERC): A new analytical frontier. *Rapid Commun Mass Spectrom*. 2019;33:1258-1266. doi: 10.1002/rcm.8462
20. Stein WH, Moore S. Amino acid composition of beta-lactoglobulin and bovine serum albumin. *J Biol Chem*. 1949;178(1):79-91.

21. Keutmann HT, Potts JT. Improved recovery of methionine after acid hydrolysis using mercaptoethanol. *Tech Rep.* 1969:175-185 doi: 10.1016/0003-2697(69)90300-5
22. Hunt S. Degradation of amino acids accompanying in vitro protein hydrolysis. *Chemistry and Biochemistry of the Amino Acids.* 1985: 376-398. doi: 10.1007/978-94-009-4832-7_12
23. MacDonald JL, Krueger MW, Keller JH. Oxidation and hydrolysis determination of sulfur amino acids in food and feed ingredients: collaborative study. *J Assoc Off Anal Chem.* 1985;68(5):826-829. doi: 10.1093/jaoac/68.5.826
24. Manneberg M, Lahm HW, Fountoulakis M. Quantification of cysteine residues following oxidation to cysteic acid in the presence of sodium azide. *Anal Biochem.* 1995;231(2):349-353. doi: 10.1006/abio.1995.9988
25. Abadie C, Tcherkez G. Plant sulphur metabolism is stimulated by photorespiration. *Communications Biology.* 2019;2(379):1-7.
26. Inglis AS, Liu TY. The stability of cysteine and cystine during acid hydrolysis of proteins and peptides. *J Biol Chem.* 1970;245(1):112-116.
27. Yano H, Aso K, Tsugita A. Further study on gas phase acid hydrolysis of protein: improvement of recoveries for tryptophan, tyrosine, and methionine. *J Biochem.* 1990;108(4):579-582. doi: 10.1093/oxfordjournals.jbchem.a123245
28. Smyth DG, Stein WH, Moore S. The sequence of amino acid residues in bovine pancreatic ribonuclease: revisions and confirmations. *J Biol Chem.* 1963;238: 227-234.
29. Guidotti G, Konigsberg W. The characterization of modified human hemoglobin I: reaction with iodoacetamide and N-ethylmaleimide. *J Biol Chem.* 1964;239(5):1474-1484.
30. Grant GA. Modification of cysteine. *Current protocols in protein science.* 2017;87:1-23. doi: 10.1002/cpps.22
31. Friedman M, Krull LH, Cavins JF. The chromatographic determination of cystine and cysteine residues in proteins as s-beta-(4-pyridylethyl)cysteine. *J Biol Chem.* 1970;245(15):3868-3871.
32. Rampler E, Dalik T, Stingeder G, Hann S, Koellensperger G. Sulfur containing amino acids – challenge of accurate quantification. *J Anal At Spectrom.* 2012;27(6):1018-1023. doi: 10.1039/C2JA10377J
33. Albert CS, Loki K, Pohn G, Varga-Visi E, Csapo J. Investigation of performic acid oxidation in case of thiol-containing amino acid enantiomers. *Acta Univ Sapientiae, Alimentaria.* 2008;1:73-80.
34. Hess S, Van Beek J, Pannell LK. Acid hydrolysis of silk fibroins and determination of the enrichment of isotopically labeled amino acids using precolumn derivatization and high-performance liquid chromatography–electrospray ionization–mass spectrometry. *Anal Biochem.* 2002;311(1):19-26. doi: 10.1016/S0003-2697(02)00402-5
35. Hayes JM. An introduction to isotope calculations. *WHOI.* 2004: 1-10.
36. Wang Y, Espenson JH. Oxidation of symmetric disulfides with hydrogen peroxide catalyzed by methyltrioxorhenium (VII). *J Org Chem.* 2000;65(1):104-107. doi: 10.1021/jo991109w
37. Cheng CN. Extracting and desalting amino acids from soils and sediments: evaluation of methods. *Soil Biol Biochem.* 1975;7(4):319-322. doi: 10.1016/0038-0717(75)90074-7

38. Amelung W, Zhang X. Determination of amino acid enantiomers in soils. *Soil Biol Biochem.* 2001;33(4):553-562. doi: 10.1016/S0038-0717(00)00195-4
39. Takano Y, Kashiwayama Y, Ogawa NO et al. Isolation and desalting with cation-exchange chromatography for compound-specific nitrogen isotope analysis of amino acids: application to biogeochemical samples. *Rapid Commun Mass Spectrom.* 2010;24(16):2317-2323. doi: 10.1002/rcm.4651
40. Epstein S, Krishnamurthy RV, Cronin JR et al. Unusual stable isotope ratios in amino acid and carboxylic acid extracts from the Murchison meteorite. *Nature.* 1987;326():477-479. doi: 10.1038/326477a0
41. McCullagh J, Gaye-Siessegger J, Focken U. Determination of underivatized amino acid $\delta^{13}\text{C}$ by liquid chromatography/isotope ratio mass spectrometry for nutritional studies: the effect of dietary non-essential amino acid profile on the isotopic signature of individual amino acids in fish. *Rapid Commun Mass Spectrom.* 2008;2:1817-1822. doi: 10.1002/rcm.3554
42. Fujii K, Ikai Y, Mayumi T et al. A nonempirical method using LC/MS for determination of the absolute configuration of constituent amino acids in a peptide: elucidation of limitations of Marfey's method and of its separation mechanism. *Anal Chem.* 1997;69(16):3346-3352. doi: 10.1021/ac9701795
43. Kochhar S, Christen P. Amino acid analysis by high-performance liquid chromatography after derivatization with 1-fluoro-2,4-dinitrophenyl-5-L-alanine amide. *Anal Biochem.* 1989;178(1):17-21. doi: 10.1016/0003-2697(89)90348-5
44. Raven MR, Sessions AL, Adkins JF et al. Rapid organic matter sulfurization in sinking particles from the Cariaco Basin water column. *Geochim Cosmochim Acta.* 2016;190:175-190. doi: 10.1016/j.gca.2016.06.030
45. Huston PL, Pignatello JJ. Degradation of selected pesticide active ingredients and commercial formulations in water by the photo-assisted Fenton reaction. *Water Research.* 1999;33(5):1238-1246. doi: 10.1016/S0043-1354(98)00330-3
46. White RH. A method for the measurement of sulfur-34 abundance in bound cysteine and methionine. *Anal Biochem.* 1981;114:349-354. doi: 10.1016/0003-2697(81)90492-9
47. Canfield DE. Biogeochemistry of sulfur isotopes. *Reviews in Mineralogy and Geochemistry.* 2001;43(1):607-636. doi: 10.2138/gsrmg.43.1.607
48. Habicht KS, Canfield DE. Isotope fractionation by sulfate-reducing natural populations and the isotopic composition of sulfide in marine sediments. *Geology.* 2001;29(6):555-558. doi: 10.1130/0091-7613(2001)029<0555:ifbsrn>2.0.co;2
49. Kaplan IR, Emery KO, Rittenberg SC. The distribution and isotopic abundance of sulphur in recent marine sediments off southern California. *Geochim Cosmochim Acta.* 1963;27:297-331. doi: 10.1016/0016-7037(63)90074-7
50. Mekhtieva VL, Pankina RG. Isotopic composition of sulfur in aquatic plants and dissolved sulfates. *Geochemistry International.* 1968;5:624-627.
51. Oduro H, VanAlsyne KL, Farquhar J. Sulfur isotope variability of oceanic DMSP generation and its contributions to marine biogenic sulfur emissions. *PNAS.* 2012;109(23):9012-9016. doi: 10.1073/pnas.1117691109
52. Peterson BJ, Howarth RW, Garritt RH. Multiple stable isotopes used to trace the flow of organic matter in estuarine food webs. *Science.* 1985;227:61-63. doi: 10.1126/science.227.4692.1361

53. Peterson BJ, Fry B. Stable isotopes in ecosystem studies. *Annu Rev Ecol Syst.* 1987;18:293-320. doi: 10.1146/annurev.es.18.110187.001453
54. Wu P, Tang L, Jiang W, et al. The relationship between dietary methionine and growth, digestion, absorption, and antioxidant status in intestinal and hepatopancreatic tissues of sub-adult grass carp (*Ctenopharyngodon idella*). *Journal of Animal Science and Biotechnology.* 2017;8(63):1-14. doi: 10.1186/s40104-017-0194-0
55. Howe K, Clark MD, Torroja CF, et al. The zebrafish reference genome sequence and its relationship to the human genome. *Nature.* 2013;496:498-503. doi: 10.1038/nature12111
56. Kwart H, Stanulonis J. Assessment of the thioallylic rearrangement by a simplified technique for high-precision measurement of isotope effects. *J Am Chem Soc.* 1976;98(13):4009-4010. doi: 10.1021/ja00429a052
57. Price MN, Zane GM, Kuehl JV et al. Filling gaps in bacterial amino acid biosynthesis pathways with high-throughput genetics. *PLOS Genetics.* 2018;15(4):1-23. doi: 10.1371/journal.pgen.1007147
58. Caspi R, Billington R, Fulcher CA, et al. The MetaCyc database of metabolic pathways and enzymes. *Nucleic Acids Research.* 2018;46(1):633-639. doi: 10.1093/nar/gkx935
59. Hwang BJ, Yeom HJ, Kim Y, Lee HS. *Corynebacterium glutamicum* Utilizes both Transsulfuration and Direct Sulfhydrylation Pathways for Methionine Biosynthesis. *Journal of Bacteriology.* 2002;184(5):1277-1286. doi: 10.1128/JB.184.5.1277-1286.2002
60. North JA, Narrowe AB, Xiong W, Byerly KM, Zhao G, Young SJ, Murali S, Wildenthal JA, Cannon WR, Wrighton KC, Hettich RL, Tabita FR. A nitrogenase-like enzyme system catalyzes methionine, ethylene, and methane synthesis. *Science.* 2020;369(6507):1094-1089. doi: 10.1126/science.abb6310

Measured species	Analytical Technique	Minimum Sample ($\mu\text{g S}$)	$\delta^{34}\text{S}$ Precision (1sd)	Parameters Measured	Ref
S^+	MC/ICPMS	0.2	0.05 - 0.10‰	$\delta^{34}\text{S}$, $\Delta^{33}\text{S}$	11
	GC/MC/ICPMS	0.001	0.1‰	$\delta^{34}\text{S}$	14
SF_6^+	IRMS (Dual-Inlet)	440	0.05‰	$\delta^{34}\text{S}$, $\Delta^{33}\text{S}$, $\Delta^{36}\text{S}$	8
	IRMS (Microvolume)	0.6	0.04 - 0.15‰	$\delta^{34}\text{S}$, $\Delta^{33}\text{S}$, $\Delta^{36}\text{S}$	9
SO_2^+	IRMS (Dual-Inlet)	640	<0.2‰	$\delta^{34}\text{S}$	6
	EA/IRMS (Conventional)	70	0.3‰	$\delta^{34}\text{S}$	7
	EA/IRMS (Purge and Trap)	35	0.4‰	$\delta^{34}\text{S}$	17
	EA/IRMS (Dual GC Column)	30	<0.2‰	$\delta^{34}\text{S}$	18
	EA/IRMS (Ramped GC Column)	2.0 1.0*	0.3‰ 0.2‰*	$\delta^{34}\text{S}$	19

Table 1: Summary of mass spectrometric methods for the determination of natural abundance sulfur isotope ratios, with reported sensitivity and precision. Asterisks indicate work in this study.

Sample	$\delta^{34}\text{S}$ Before (0.3‰)	$\delta^{34}\text{S}$ After (0.3‰)
Cysteine	5.8	5.6
Methionine	7.4	7.6
Bovine Serum Albumin	1.5	Cysteic Acid: 1.9 Methionine Sulfone: 1.9

Table 2: $\delta^{34}\text{S}$ values of amino acid and protein standards measured before and after sample workup.

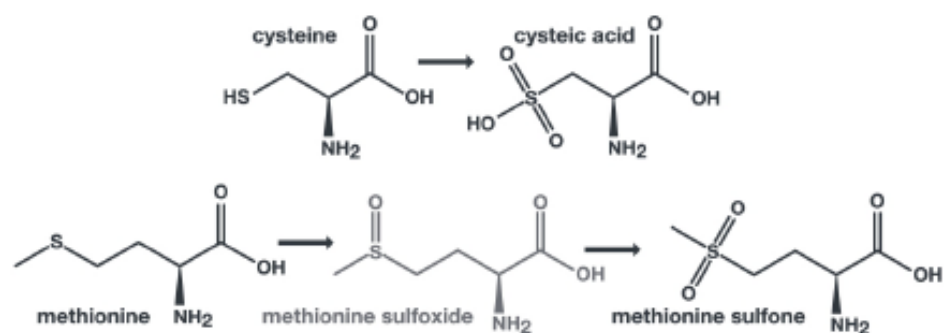


Figure 1: Progressive oxidation of the amino acids cysteine and methionine. Although cysteine has intermediate oxidation states, the sulfonic acid endmember (cysteic acid) is most stable and so is the common oxidation product. In contrast, methionine oxidation often yields several products including methionine sulfoxide and methionine sulfone. Such uncontrolled oxidation reactions have hampered many previous efforts at quantification and/or isolation of the sulfur amino acids.

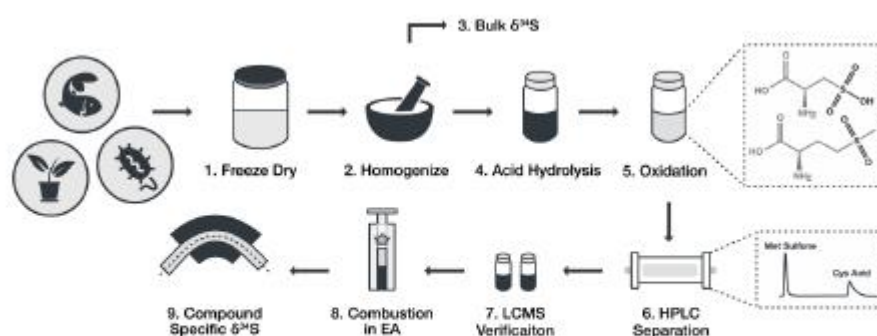


Figure 2: A flowchart of the overall approach to sulfur isotope analysis of cysteine and methionine from biological samples.

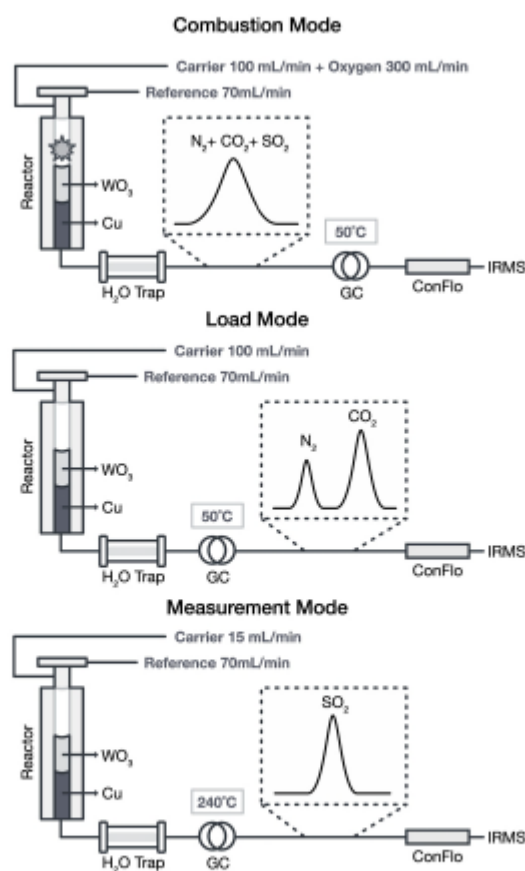


Figure 3: Schematic illustration of sulfur isotope measurement using a Thermo Fisher™ Scientific Flash EA IsoLink™ CN connected to an Isotope Ratio Mass Spectrometer. In load mode, SO_2 remains on the GC column, while N_2 and CO_2 elute, SO_2 is released in measurement mode, when the GC temperature ramps to 240°C and carrier gas rate flow drops to 15 mL/min .

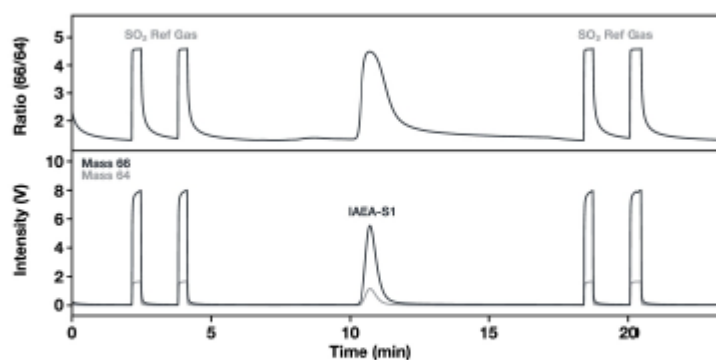


Figure 4: Representative chromatogram for an EA-IRMS acquisition. Total run time is 24 min. Here, the sample is $37\text{ }\mu\text{g}$ of the silver sulfide standard IAEA-S1 ($4.8\text{ }\mu\text{g S}$). 1 V intensity for $m/z\ 64$ corresponds to a 3.3 nA ion current.

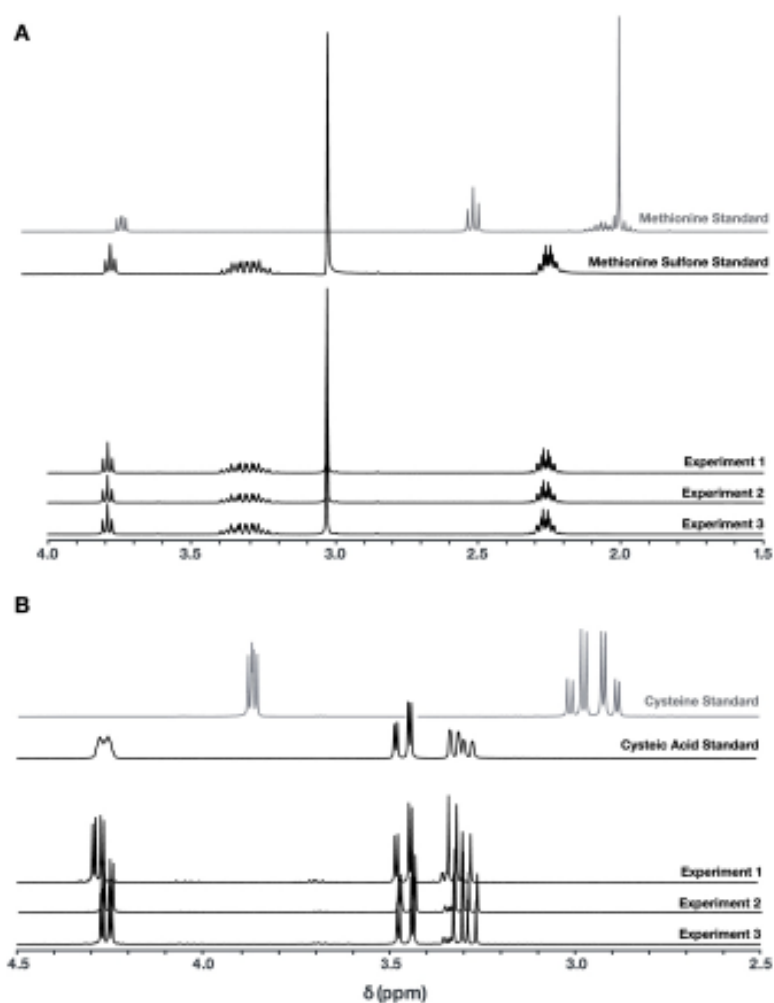


Figure 5: ¹H NMR spectra of the performic acid oxidation of cysteine to cysteic acid (top) and methionine to methionine sulfone (bottom). Experiments were conducted in triplicate (displayed here as stacked spectra). Reference spectra are seen above. In each case, NMR profiles were unambiguously assigned to the oxidized species, with no detectable cysteine, methionine, or methionine sulfoxide.

Accepted

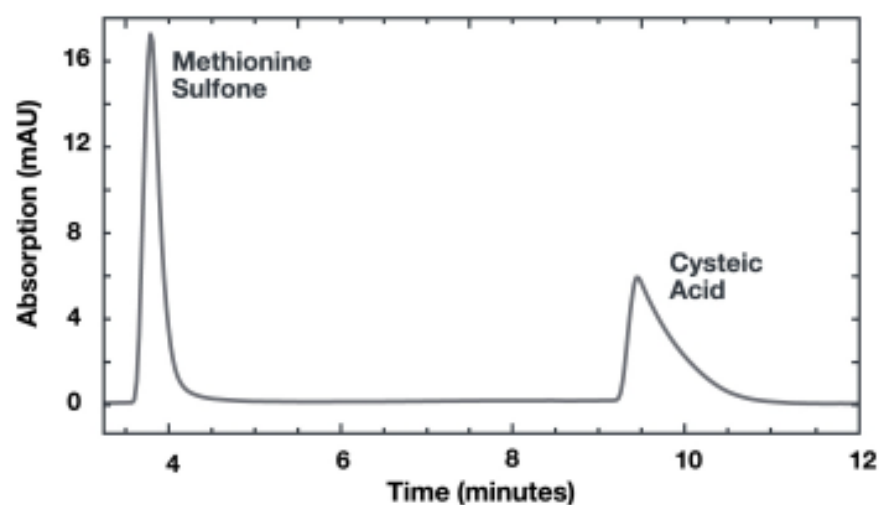


Figure 6: HPLC-UV chromatogram showing separation of cysteic acid and methionine sulfone standards on the PRP-X100 column. The 20 min isocratic method uses 50 mM ammonium acetate buffered to pH 8 as the mobile phase, with UV absorption measured at 254 nm.

Accepted

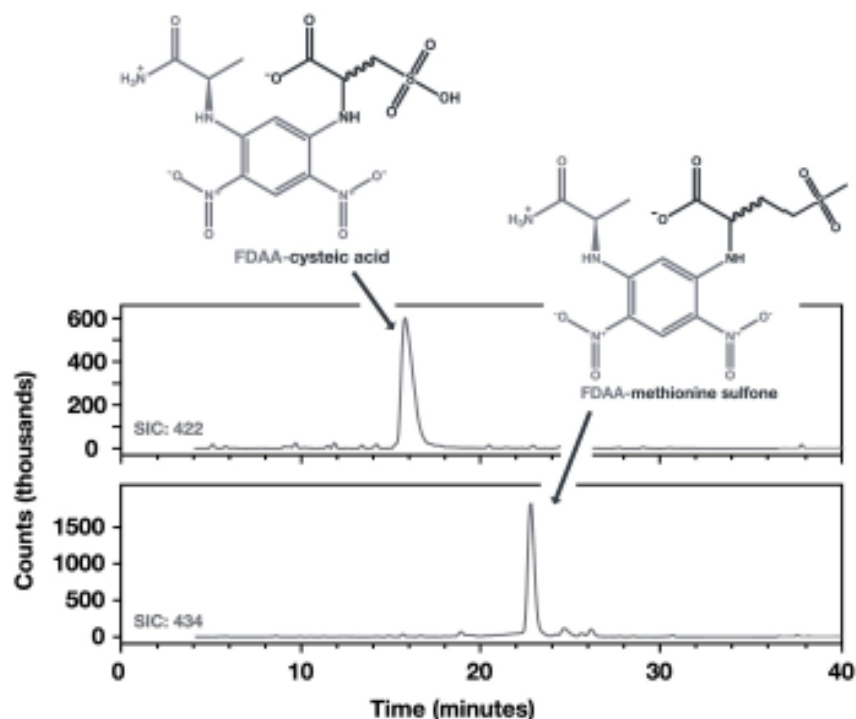


Figure 7: LC/MS selected-ion chromatograms of cysteine acid (top) and methionine sulfone (bottom) from collected fractions of the HPLC separation. Aliquots were derivatized with FDAA (1-fluoro-2,4-dinitrophenyl-5-L-alanine amide). Derivatized cysteine acid and methionine sulfone were identified via selected ion chromatograms at m/z 422 and 434, respectively.

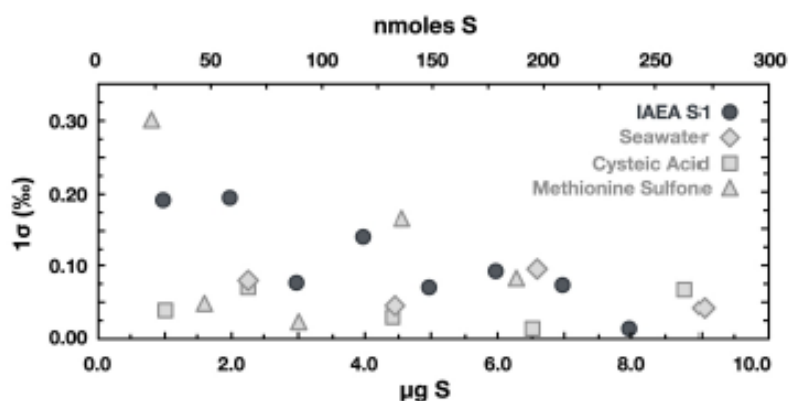


Figure 8: Precision (1 s.d.) of triplicate analyses of $\delta^{34}\text{S}$ for pure standards of cysteine acid, methionine sulfone, silver sulfide (IAEA-S1), and seawater sulfate analyzed by EA/IRMS. Sulfur in seawater is present almost entirely as dissolved sulfate.

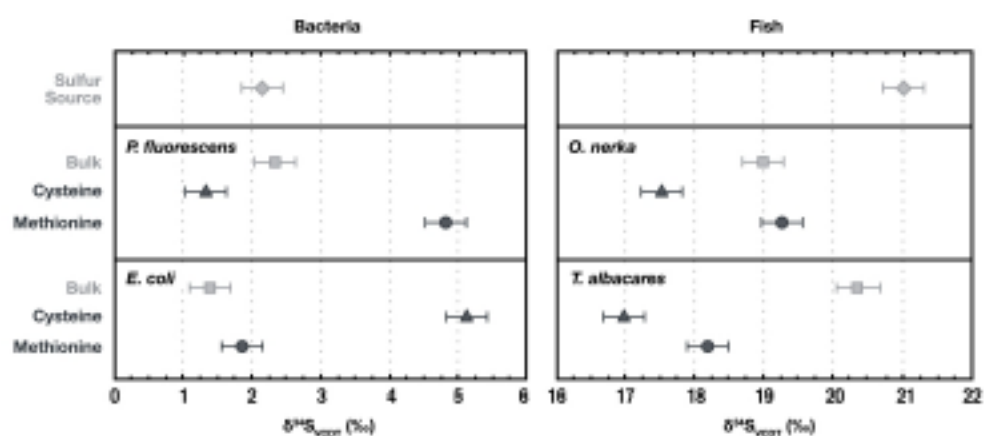


Figure 9: $\delta^{34}\text{S}$ values of cysteine (measured as cysteic acid), methionine (measured as methionine sulfone), bulk bacterial/fish muscle biomass, and sulfur source for bacteria (A) and fish (B). For bacteria, the sulfur source was ammonium sulfate added to the culture medium, which was measured directly on the EA/IRMS. The indirect sulfur source for fish was inferred to be marine sulfate ($\delta^{34}\text{S} = 21\text{‰}$) for both species.

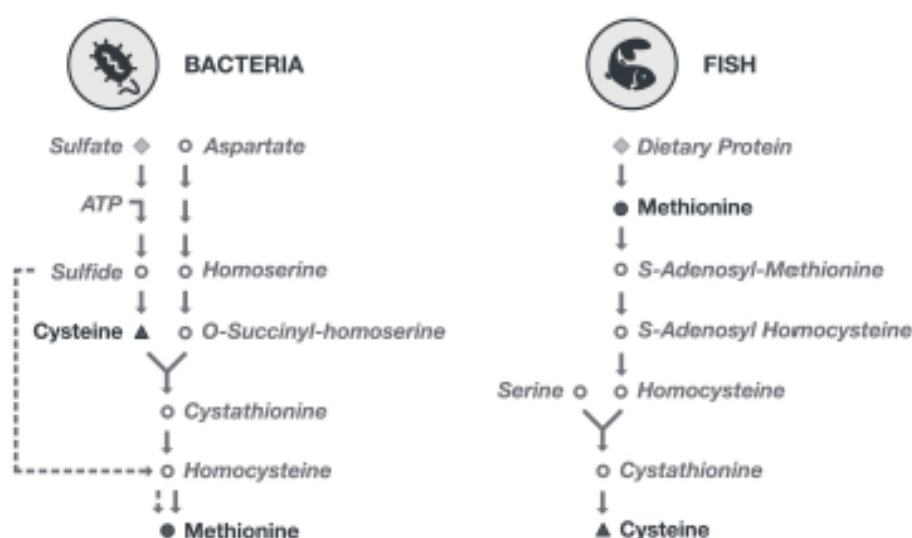


Figure 10: Known sulfur assimilation pathways in A) bacteria and B) fish. Note that the fish metabolism shown is from the closest living organism for which the pathway is well studied, *Danio rerio* (zebrafish). Solid arrows in the bacterial pathway are taken from the *E. coli* MetaCyc database and show the ubiquitous methionine synthesis pathway via transsulfuration. The dashed arrow represents an alternative route via sulfhydrylation where methionine is synthesized directly from sulfide via homocysteine. Sulfhydrylation is not present in *E. coli* but has been found in diverse bacteria including *P. putida* and *B. subtilis*.

Accepted